



OPEN

## Anthropogenic nutrient loads and season variability drive high atmospheric N<sub>2</sub>O fluxes in a fragmented mangrove system

N. Regina Hershey<sup>1,2</sup>, S. Bijoy Nandan<sup>2✉</sup>, K. Neelima Vasu<sup>2</sup> & Douglas R. Tait<sup>3,4</sup>

Fragmented mangroves are generally ignored in N<sub>2</sub>O flux studies. Here we report observations over the course of a year from the Mangalavanam coastal wetland in Southern India. The wetland is a fragmented mangrove stand close to a large urban centre with high anthropogenic nitrogen inputs. The study found the wetland was a net source of N<sub>2</sub>O to the atmosphere with fluxes ranging between 17.5 to 117.9  $\mu\text{mol m}^{-2} \text{day}^{-1}$  which equated to high N<sub>2</sub>O saturations of between 697 and 1794%. The average dissolved inorganic nitrogen inputs ( $80.1 \pm 18.1 \mu\text{mol L}^{-1}$ ) and N<sub>2</sub>O emissions ( $59.2 \pm 30.0 \mu\text{mol m}^{-2} \text{day}^{-1}$ ) were highest during the monsoon season when the rainfall and associated river water inputs and terrestrial runoff were highest. The variation in N<sub>2</sub>O dynamics was shown to be driven by the changes in rainfall, water column depth, salinity, dissolved oxygen, carbon, and substrate nitrogen. The study suggests that fragmented/minor mangrove ecosystems subject to high human nutrient inputs may be a significant component of the global N<sub>2</sub>O budget.

Increasing anthropogenic terrestrial nitrogen (N) inputs and sewage pollution is regarded as one of the major cause for N enrichment in coastal wetlands. Coastal wetlands, estuaries and adjoining mangrove fringes which are in close proximity to human settlements can act as important sinks of terrestrial N where it can be stored and cycled. It is reported that 1% of reactive nitrogen entering estuaries are released as nitrous oxide (N<sub>2</sub>O) emissions<sup>1</sup>. N<sub>2</sub>O is a major contributor to stratospheric ozone depletion, has a lifetime of 118–131 years in the atmosphere<sup>2</sup> and has about 300 times greater global warming potential than carbon dioxide (CO<sub>2</sub>)<sup>3</sup>. N<sub>2</sub>O is produced as an intermediate product during the denitrification process (heterotrophic NO<sub>3</sub> reduction) and also as a by-product during the nitrification process (autotrophic oxidation of NH<sub>4</sub> to NO<sub>3</sub>) and it is consumed during complete denitrification of N<sub>2</sub>O via dissimilatory reduction to N<sub>2</sub><sup>4</sup>. Therefore, the ratio of production and consumption of N<sub>2</sub>O determines whether these coastal wetlands are sinks or sources of N<sub>2</sub>O. However, the production and consumption of N<sub>2</sub>O in a system is determined by several drivers such as temperature, pH, dissolved oxygen (DO), carbon (C) and hydrologic parameters in the environment<sup>4</sup>.

Mangroves increase the ecosystem value of coastal wetlands through their significant role in nutrient cycling, moderation of extreme weather events, supply of food and raw materials, and provision of breeding, spawning and nursery habitat for a variety of invertebrates and commercial fish species. However, the effectiveness of mangroves to meet these services is affected by the degree of anthropogenic disturbance. Recent studies have shown that tropical mangrove wetlands are under high risk from anthropogenic stresses particularly due to the extensive use of terrestrial N fertilizers causing dissolved inorganic nitrogen (DIN) enrichment<sup>5,6</sup>. Major mangrove ecosystems around the globe have been assessed for their contribution to atmospheric N<sub>2</sub>O budgets. However, despite our knowledge about the contribution of mangrove wetlands in the global N<sub>2</sub>O budget, uncertainties still exist due to lack of information about the impact of fragmented mangrove wetlands which are numerous in the tropical regions and particularly along the Indian coastline. As tropical areas receive disproportionately more rainfall than temperate areas, this likely leads to greater terrestrial N into coastal wetlands from nearby urban and agricultural areas. The high seasonal variability in rainfall distribution patterns in tropical areas may also drive large temporally variability in coastal N<sub>2</sub>O dynamics.

<sup>1</sup>Department of Zoology, N.S.S. Hindu College, Changanassery 686 102, India. <sup>2</sup>Department of Marine Biology, Microbiology and Biochemistry, School of Marine Sciences, Cochin University of Science and Technology, Cochin 682 016, India. <sup>3</sup>Faculty of Environment and Science, Southern Cross University, Lismore, NSW 2480, Australia. <sup>4</sup>National Marine Science Centre, Southern Cross University, PO Box 4321, Coffs Harbour, NSW 2450, Australia. ✉email: bijoynandan@yahoo.co.in

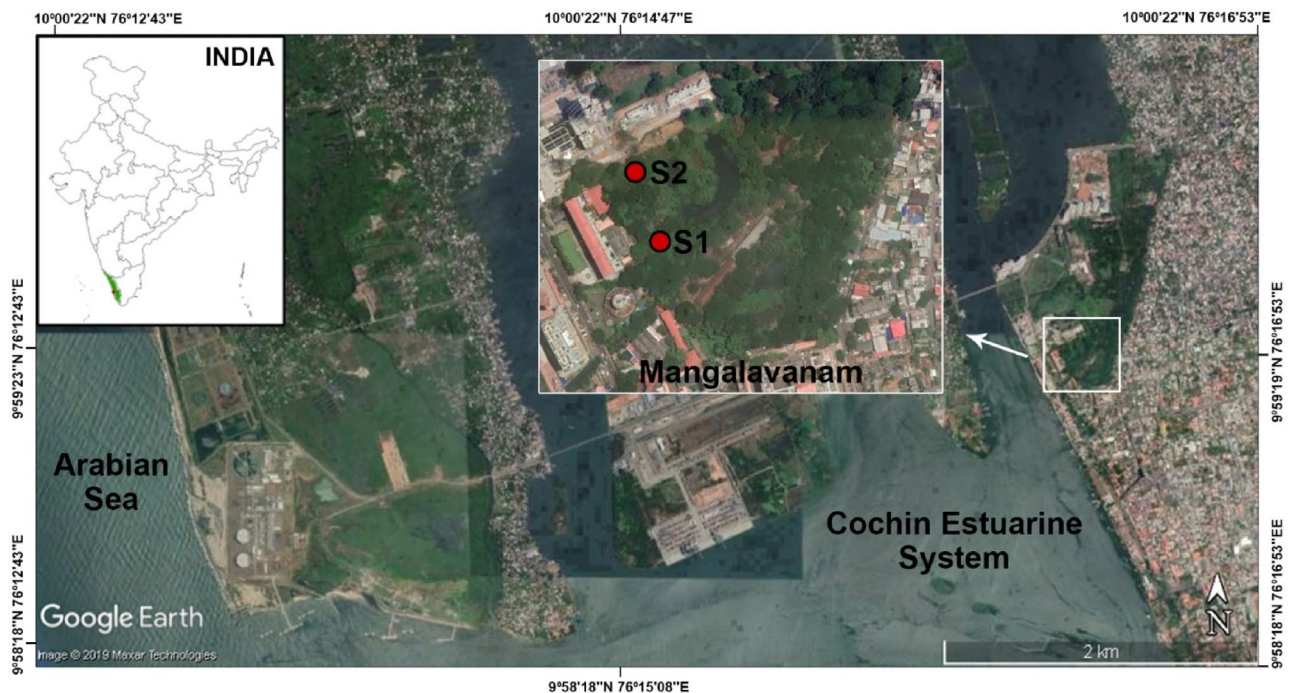


**Figure 1.** Map of Mangalavanam Coastal Wetland, Kerala, India depicting the study stations [source: Google earth pro V 7.3. (November 12, 2019). Kochi, Kerala.  $9^{\circ} 59' 23.83''$  N,  $76^{\circ} 16' 26.74''$  E, Eye alt 7.6 km. [Along the Indian coast \(7,516.6 km long<sup>7</sup>\), mangrove cover an area of 497,500 ha<sup>8</sup>. The India state Kerala in southern India, was once rich in mangrove habitats, but the area of intact mangrove has drastically declined due to anthropogenic pressures such as urbanisation, burgeoning power projects and rapid industrialisation. It is estimated that the Ernakulum district in Kerala has 943 mangrove stands of which 880 \(~93%\) of them have an area less than 1 hectare. The contribution of these smaller mangrove systems is often ignored and their role in global nutrient cycling has yet to be adequately determined. As most of these mangrove stands are generally observed near the vicinity of human settlements, they can be critically influenced by the N loading there. Recent global studies suggest that aquatic environments influenced by intensive agricultural practices and industrial activities can act as source of  \$N\_2O\$  to the atmosphere<sup>9–11</sup> and this predicted rise in terrestrial N concentrations can potentially triple the global  \$N\_2O\$  emissions from coastal wetlands<sup>1</sup>. However, Indian mangrove stands have been mostly ignored from the N input and output studies due to their relatively smaller area and footprint. The few studies that have taken place in Indian mangroves suggest that they are highly influenced by anthropogenic nutrient inputs and are significant sources of atmospheric  \$N\_2O\$ <sup>12–14</sup>. In light of the increasing anthropogenic N inputs, it is important to monitor and assess the potential of fragmented/minor mangrove stands for their contribution of  \$N\_2O\$  to the atmosphere.](https://earth.google.com/web/search/Mangalavanam+Bird+Sanctuary,+High+Court+Road,+Ayyappankavu,+Kochi,+Kerala,+India/@9.9893564,76.2747626,4.86064735a,2322.96914379d,35y,240.09539944h,45t,0r/data=Cr0BGpIBEosBCiUweDNiMDgwZDU5Mjk0ZWQxZDU6MHhlMjcwYmIzMGIwZGY3OGYwGTUtDOyM-iNAIX5K37WVEVNAKIBNYW5nYwXhdmFuYW0gQmlyZCBTYW5jdHVhcncsIEhpZ2ggQ291cnQgUm9hZCwgQXI5YXBwYW5rYXZlLCBib2NoaSwgS2VyYWxhLCBjbmRyYRgCIAEijgokCf0tW8UnikNAEZyxdwYtjXAGXdpXswSvVxAISISbeKakktA].</a></p>
</div>
<div data-bbox=)

In order to understand the contribution of fragmented/minor mangrove stands to atmospheric  $N_2O$  emissions, this study aimed to assess the Mangalavanam Coastal Wetland (MCW) a fragmented minor mangrove stand adjacent to the city of Kochi, India over a one year period incorporating a range of distinct seasons. The  $N_2O$  flux rates were calculated using three different k models<sup>15–17</sup> to reduce the uncertainty in calculated  $N_2O$  flux rates. The study also tested the relation between N substrates and  $N_2O$  fluxes with temperature, pH, DO, and C loading of the wetland to determine the drivers of  $N_2O$  dynamics.

**Study area.** The MCW is a semi-closed fragmented mangrove stand in the Ernakulum district along the south-west coast of India at  $9^{\circ} 59' 23.83''$  N and  $76^{\circ} 16' 26.74''$  E (Fig. 1). It receives tidal input through a narrow channel/feeder canal from the adjacent nutrient rich Cochin Estuarine System (CES), where eutrophication is of great concern<sup>18</sup>. This tidal wetland has a wet and maritime tropical climate with three distinct seasons: pre-monsoon (February to May), southwest monsoon (June to September, from here on called monsoon) and northeast monsoon (October to January) or post-monsoon. The wetland is relatively shallow (<0.5 m) and is largely inundated during high tide flooding. The dominant mangrove species present in the MCW are *Rhizophora mucronata*, *Avicennia officinalis* and *Acanthus ilicifolius*. Mangrove associates such as *Acrostichum aureum*, *Deris trifoliata* and *Morinda citrifolia* are also common. Kochi is the most densely inhabited city in Kerala with an

urban population of more than of 2.1 million in an area of 440 km<sup>2</sup>. The MCW receives nutrient input from the urban drainage systems of the adjacent human settlements. Due to government restrictions on sampling in the area, only two sites could be sampled, a site heavily influenced by upstream estuarine inputs (Site 1) and a relatively pristine site (Site 2).

## Results

**Physico-chemical attributes.** The area received 3469 mm of rainfall over the study period, with 68.5% falling during the monsoon season (2376 mm) (Fig. 2, Table 1). The mean wind speed of the study area was  $2.4 \pm 0.4$  m s<sup>-1</sup>, with monthly averages ranging from 2.0 m s<sup>-1</sup> in April to 3.2 m s<sup>-1</sup> in June. The wetland depth was generally shallow, with a mean depth of  $0.3 \pm 0.8$  m and ranged from 0.1 m in February to 0.5 m in June. The mean annual water and sediment temperature was  $27.0 \pm 0.9$  °C and  $27.4 \pm 0.8$  °C, respectively. The mean mixo-mesohaline to mixo-polyhaline salinity was  $12.3 \pm 7.2$  ‰, with significant differences between seasons ( $f=107.20$ ,  $\rho < 0.001$ ). The mean DO concentrations in the water column was  $112.2 \pm 45.6$  µmol L<sup>-1</sup> and decreased from the post-monsoon season ( $156.1 \pm 16.0$  µmol L<sup>-1</sup>) to the pre-monsoon season ( $109.0 \pm 30.1$  µmol L<sup>-1</sup>), and to the monsoon season ( $71.6 \pm 39.8$  µmol L<sup>-1</sup>). The annual mean DO saturation was  $229.2 \pm 11.2\%$  and AOU was  $117.0 \pm 45.7$  µmol L<sup>-1</sup> with both varying significantly between seasons ( $f=32.00$ ,  $\rho < 0.001$  and  $f=16.36$ ,  $\rho < 0.001$ , respectively). The pH of the water column over the year ranged from 6.5 to 7.6 with a mean of  $6.8 \pm 0.3$ , while in the sediments it ranged from 6.1 to 6.7. There was a significant difference in pH in the water column between seasons ( $f=9.07$ ,  $\rho=0.002$ ) and in sediment pH between stations ( $f=4.72$ ,  $\rho=0.043$ ).

**Carbon and nitrogen measurements.** The total nitrogen (TN) concentration in the water column ranged from 172.1 to 877.1 µmol L<sup>-1</sup>, with an annual mean of  $399.4 \pm 244.8$  µmol L<sup>-1</sup> and in the sediments it ranged from 158.6 to 301.4 µmol g<sup>-1</sup> (Table 1). The mean TN in the water column was highest during the monsoon season and the lowest during post-monsoon season, while in sediments the maximum concentration was observed during the post-monsoon season and the minimum during the pre-monsoon season. Dissolved nitrogen (DN) contributed 66 to 88% of the observed TN with an annual mean of  $322.1 \pm 182.0$  µmol L<sup>-1</sup> and varied significantly on temporal basis ( $f=9.16$ ,  $\rho=0.002$ ). Dissolved inorganic nitrogen constituted 12–41% of the DN concentrations with an annual mean of  $60.7 \pm 18.1$  µmol L<sup>-1</sup>, while DON was 58–88% of the DN concentration with an annual mean of  $248.6 \pm 168.9$  µmol L<sup>-1</sup>. The DIN and DON concentrations in the water column varied significantly on seasonal basis ( $f=17.15$ ,  $\rho < 0.001$  and  $f=8.26$ ,  $\rho=0.003$ , respectively) with higher DIN and DON in the monsoon season. NO<sub>3</sub> was the major constituent of DIN, with a mean of  $62 \pm 8\%$  of DIN. NO<sub>3</sub> was followed by NH<sub>4</sub> and NO<sub>2</sub>, constituting about 36 ± 8% and 2 ± 1%, of the DIN respectively. There was a significant difference in water column NH<sub>4</sub> ( $f=8.89$ ,  $\rho=0.002$ ), NO<sub>2</sub> ( $f=15.47$ ,  $\rho < 0.001$ ) and NO<sub>3</sub> ( $f=11.89$ ,  $\rho=0.001$ ) seasonally. Particulate nitrogen (PN) in the water column ranged from 20.1 µmol L<sup>-1</sup> to 232.9 µmol L<sup>-1</sup> during the study period and varied significantly between seasons ( $f=8.76$ ,  $\rho=0.002$ ). The total carbon (TC) concentration in the water column ranged from 2473.3 to 7391.7 µmol L<sup>-1</sup> (average  $3916.3 \pm 1453.0$  µmol L<sup>-1</sup>) with total organic carbon (TOC) contributing 33 ± 10% of the observed TC concentrations (range from 484.2 to 3792.5 µmol L<sup>-1</sup>) which varied significantly on seasonal basis ( $f=4.63$ ,  $\rho=0.02$ ). In the sediment, TOC concentrations ranged between 2877.5 µmol g<sup>-1</sup> to 9911.7 µmol g<sup>-1</sup> over the study period. In the water column, the mean TOC concentration was highest during the monsoon season and lowest during the post-monsoon season, while in sediments, the maximum concentration was observed during the post-monsoon season ( $6230.3 \pm 2292.4$  µmol g<sup>-1</sup>) and the minimum concentration was observed during the pre-monsoon season ( $4000.8 \pm 1323.8$  µmol g<sup>-1</sup>). The total inorganic carbon was the major constituent of TC in the water column, with an annual mean of  $2556.4 \pm 771.6$  µmol L<sup>-1</sup>, ranged from 1578.3 µmol L<sup>-1</sup> in July to 4605.0 µmol L<sup>-1</sup> in November and varied significantly between seasons ( $f=7.57$ ,  $\rho=0.003$ ).

**Nitrous oxide dynamics.** The dissolved N<sub>2</sub>O concentration in the water column of the MCW ranged from 50.3 nM in November to 131.5 nM in June (Fig. 3, Table 1). The mean percentage saturation of N<sub>2</sub>O was  $1088 \pm 252\%$  and ranged from 696 to 1794%, with relatively little seasonal variations. Using Wanninkhof<sup>15</sup> k values, N<sub>2</sub>O fluxes ranged from 17.5 to 117.9 µmol m<sup>-2</sup> day<sup>-1</sup>, with an annual mean of  $39.1 \pm 22.6$  µmol m<sup>-2</sup> day<sup>-1</sup>. For comparisons sake, the flux calculations of Raymond and Cole<sup>17</sup>, N<sub>2</sub>O fluxes ranged from 47.7 to 207.9 µmol m<sup>-2</sup> day<sup>-1</sup>, with an annual mean of  $88.6 \pm 33.6$  µmol m<sup>-2</sup> day<sup>-1</sup> and Wanninkhof and McGillis<sup>16</sup> N<sub>2</sub>O fluxes ranged from 3.4 to 34.3 µmol m<sup>-2</sup> day<sup>-1</sup>, with an annual mean of  $9.26 \pm 7.27$  µmol m<sup>-2</sup> day<sup>-1</sup>. Using Wanninkhof<sup>15</sup> and Wanninkhof and McGillis<sup>16</sup>, the N<sub>2</sub>O flux varied significantly on seasonal basis ( $f=6.53$ ,  $\rho=0.007$  and  $f=7.55$ ,  $\rho=0.004$ , respectively), while no significant variation was observed with the N<sub>2</sub>O flux that was calculated using Raymond and Cole<sup>17</sup> calculated fluxes ( $f=3.43$ ,  $\rho=0.055$ ). The N<sub>2</sub>O flux calculated using the three models was highest during the monsoon season and lowest during the post-monsoon season.

## Discussion

This study found that the MCW fragmented mangrove stand is a C and N rich environment which favours substantial N<sub>2</sub>O production and its release into the atmosphere. The N pool and the atmospheric flux of N<sub>2</sub>O in the MCW ( $39.1 \pm 22.6$  µmol m<sup>-2</sup> day<sup>-1</sup>) was found to be higher than that reported in the adjacent CES ( $11.4 \pm 6.9$  µmol m<sup>-2</sup> day<sup>-1</sup>) where there are significant anthropogenic N inputs<sup>19</sup>. In the Bhitarkanika mangrove on the east coast of India<sup>12</sup>, high N<sub>2</sub>O emissions were observed ( $5\text{--}113.38$  µmol m<sup>-2</sup> day<sup>-1</sup>) driven by high anthropogenic nutrient loading. In other Indian mangroves—Muthupet mangrove in southern India, comparatively low N<sub>2</sub>O emissions ( $9.3\text{--}18.18$  µmol m<sup>-2</sup> day<sup>-1</sup>) were reported even though the mangrove is subjected to a range of anthropogenic inputs including aquaculture (shrimp-farming effluent) and seasonal agricultural run-off<sup>13</sup>. Our

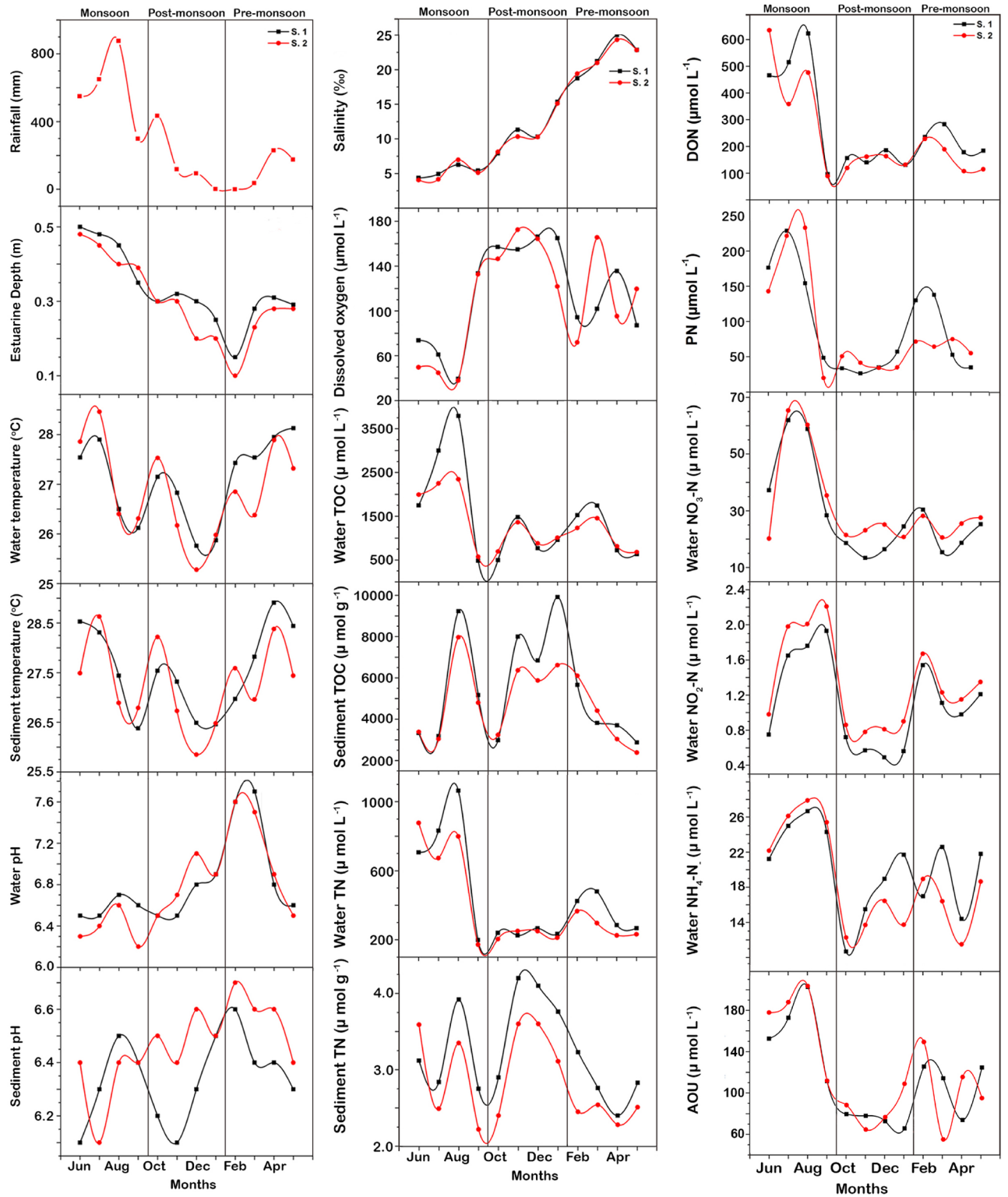


**Figure 2.** Variation in environmental parameters observed in the Mangalavanam Coastal Wetland, India during the study.

observations were also in the range of previous studies from the large eutrophic Pearl River Estuary in China ( $37 \pm 15 \mu\text{mol m}^{-2} \text{day}^{-1}$ ) which receives extensive urban, industrial and agricultural run-off<sup>10</sup>.

In a range of pristine mangroves in Australia<sup>20</sup>, the uptake of N<sub>2</sub>O has been reported with an uptake rate of  $1.52 \pm 0.17 \mu\text{mol m}^{-2} \text{day}^{-1}$ . However, the relative pristine mangrove site selected in our study (Site 2) was supersaturated with dissolved N<sub>2</sub>O ( $1122.8 \pm 266.9\%$ ) and acted as atmospheric source of N<sub>2</sub>O ( $41.0 \pm 26.1 \mu\text{mol m}^{-2} \text{day}^{-1}$ ). A recent study on N<sub>2</sub>O dynamics from four southern hemisphere subtropical

Parameters	Monsoon	Post-monsoon	Pre-monsoon
Rainfall (mm)	594.0 ± 239.7	162.4 ± 188.3	110.8 ± 109.4
Wind speed (m s <sup>-1</sup> )	2.9 ± 0.3	2.2 ± 0.1	2.2 ± 0.3
Estuarine depth (m)	0.4 ± 0.1	0.3 ± 0.1	0.2 ± 0.1
Water temperature (°C)	28.2 ± 0.5	26.6 ± 0.6	28.8 ± 0.8
Sediment temperature (°C)	29.6 ± 0.9	26.9 ± 0.8	27.8 ± 0.7
Salinity (‰)	5.2 ± 1.0	11.1 ± 2.8	21.9 ± 2.2
DO (μmol L <sup>-1</sup> )	71.6 ± 39.8	156.1 ± 16.0	109.0 ± 30.1
DO saturation (%)	236.6 ± 7.5	235.4 ± 3.7	215.6 ± 4.7
AOU (μmol L <sup>-1</sup> )	165.1 ± 36.9	79.3 ± 14.2	106.7 ± 30.5
Water pH	6.6 ± 0.1	6.7 ± 0.2	7.0 ± 0.4
Sediment pH	6.3 ± 0.2	6.4 ± 0.2	6.5 ± 0.1
Water TN (μmol L <sup>-1</sup> )	640.5 ± 289.7	235.5 ± 20.8	322.1 ± 92.3
Water DN (μmol L <sup>-1</sup> )	487.4 ± 226.5	196.3 ± 25.2	244.4 ± 63.6
Water PN (μmol L <sup>-1</sup> )	153.1 ± 81.1	39.2 ± 10.1	77.7 ± 36.9
Water DON (μmol L <sup>-1</sup> )	407.3 ± 213.3	148.5 ± 22.0	190.0 ± 59.5
Water DIN (μmol L <sup>-1</sup> )	80.1 ± 18.1	47.8 ± 10.4	54.4 ± 12.7
Water NH <sub>4</sub> (μmol L <sup>-1</sup> )	25.7 ± 2.4	19.1 ± 4.7	18.9 ± 4.9
Water NO <sub>2</sub> (μmol L <sup>-1</sup> )	1.7 ± 0.5	0.7 ± 0.2	1.3 ± 0.2
NO <sub>3</sub> (μmol L <sup>-1</sup> )	52.7 ± 15.2	27.9 ± 5.6	34.2 ± 7.5
Sediment TN (μmol g <sup>-1</sup> )	3.0 ± 0.6	3.5 ± 0.6	2.6 ± 0.3
Water TC (μmol L <sup>-1</sup> )	5255.6 ± 1995.5	3048.3 ± 704.3	3444.8 ± 921.2
Water TOC (μmol L <sup>-1</sup> )	2023.5 ± 1120.7	956.3 ± 329.7	1099.9 ± 440.3
Water TIC (μmol L <sup>-1</sup> )	3232.1 ± 874.9	2092.1 ± 374.63	2344.9 ± 480.9
Sediment TOC (μmol g <sup>-1</sup> )	5013.1 ± 2368.9	6230.3 ± 2292.4	4000.8 ± 1323.8
Dissolved N <sub>2</sub> O (nM)	80.2 ± 26.6	74.6 ± 14.0	73.2 ± 11.7
N <sub>2</sub> O saturation (%)	1103.0 ± 356.6	1022.6 ± 190.8	1137.9 ± 194.7
N <sub>2</sub> O flux, Wanninkhof, 1992 (μmol m <sup>-2</sup> day <sup>-1</sup> )	59.2 ± 30.0	28.0 ± 5.9	30.2 ± 6.9
N <sub>2</sub> O flux, Raymond and Cole, 2001 (μmol m <sup>-2</sup> day <sup>-1</sup> )	112.6 ± 48.4	74.7 ± 14.9	78.5 ± 12.1
N <sub>2</sub> O flux, Wanninkhof and McGillis, 1999 (μmol m <sup>-2</sup> day <sup>-1</sup> )	16.0 ± 9.4	5.5 ± 1.3	6.2 ± 2.2

**Table 1.** Variation in selected environmental parameters observed in the Mangalavanam Coastal Wetland, India during the study.

estuaries<sup>11</sup> (an urbanised estuary, mixed, urban and agricultural estuary and pristine estuary) reported that the N<sub>2</sub>O saturation ranged from 77.7 to 381.5% with highest saturations in the pristine estuary and lowest in the agricultural estuary, which was much lower than the range seen in this study (696.7–1794.3%). The study also reported that estuaries in the two urbanised catchments had the highest mean N<sub>2</sub>O flux rates during summer (18.8 ± 11.6 μmol m<sup>-2</sup> day<sup>-1</sup> and 18.7 ± 12.8 μmol m<sup>-2</sup> day<sup>-1</sup>, respectively) with the pristine estuary having a summer flux rate of 5.1 ± 6.9 μmol m<sup>-2</sup> day<sup>-1</sup>. Other studies from estuaries in urbanised catchments have reported low mean N<sub>2</sub>O flux rates, with 4.0 μmol m<sup>-2</sup> day<sup>-1</sup> reported in the Yarra River in Melbourne<sup>21</sup>, and 7.3 μmol m<sup>-2</sup> day<sup>-1</sup> in the Brisbane River<sup>22</sup>. The high flux rates observed here are likely a result of high rainfall in the tropics driving higher freshwater inputs, terrestrial runoff and the enhanced anthropogenic N enrichment compared to other estuaries cited above. The pristine site (Site 2) also received tidal inputs from the nutrient enriched CES which would lead to higher N<sub>2</sub>O concentrations in the water column compared to Site 1 that was heavily influenced by upstream estuarine inputs. Also, the water column of Site 1 drains out completely into the CES during low tides; however the water column depth of Site 2 was less affected during low tides which likely reduced the export of N to adjacent waters.

Significant uncertainties exist in global N<sub>2</sub>O budget due in part to the differences in methods used in calculating flux rates. Two meta-analyses published in the past 20 years highlight that the lack of direct measurements of *k* significantly hampers the ability to parameterize air–water gas exchange in estuaries and that care should be given when choosing values of *k*, with respect to location-dependent controls on gas exchange<sup>17,23</sup>. Here we offer a comparison of the different flux rates calculated using three different and commonly used *k* value models (Table 1) and the relationship of various measured parameters to N<sub>2</sub>O flux rates calculated using three models (Table 2). The parameterization of Raymond and Cole<sup>17</sup> is widely used for rivers and streams, where the turbulence reaching the air–water interface is chiefly generated by friction with the bottom. The parameterization of Wanninkhof and McGillis<sup>16</sup> is best used for open water bodies but can underestimate N<sub>2</sub>O flux rates where wind speeds are low such as sheltered mangrove systems. The *k* value model of Wanninkhof<sup>15</sup> is also commonly used and uses the Schmidt number of the water related to viscosity and with its exponent reflecting the surface layer's rate of turbulent renewal. As water column depth, wind speed, and current velocity act as main drivers of these *k* models and influences turbulence at the air–water interface, in shallow flowing ecosystems<sup>24,25</sup>, such as in mangroves, we felt the *k* value model of Wanninkhof<sup>15</sup> best fits for the study.

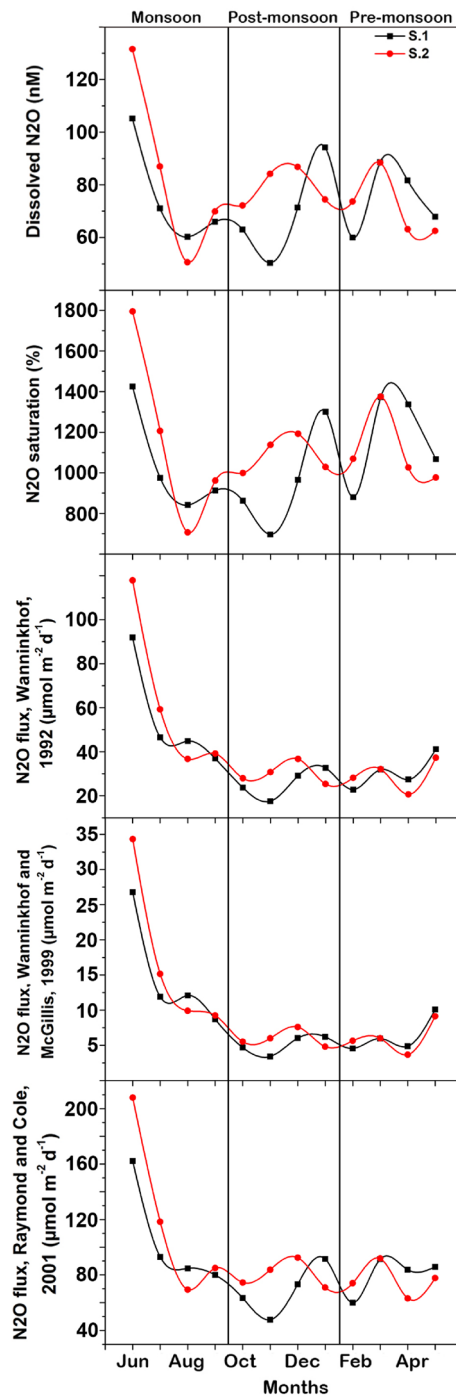


**Figure 3.** Variation in N<sub>2</sub>O dynamics observed in the Mangalavanam Coastal Wetland, India during the study.

The study observed a relationship between N<sub>2</sub>O dynamics and the availability of nitrogen species (Table 2). Concentrations of TN, DN, DON, NO<sub>3</sub>, NH<sub>4</sub> and NO<sub>2</sub> in the study area were high and at the high end of the range of concentrations seen in other highly polluted estuaries<sup>26</sup>. MCW is located in the heart of the densely populated Kochi city and has several sewage inlets from surrounding human settlements. This significantly increases the availability of N in both sediments and the water column leading to higher N<sub>2</sub>O production in the study area. Recent studies have shown that sewage influxes increase N<sub>2</sub>O production<sup>19,22</sup>. The release of nitrogenous compounds through the excreta of water-birds can also cause N enrichment in mangroves<sup>26</sup> and the abundant water bird population of MCW would also lead to higher nitrogen loads in the study sites.

The MCW also receives significant N inputs through the narrow channel from CES that receives substantial fresh water discharge (approx.  $1.2 \times 10^{10}$  m<sup>3</sup> year<sup>-1</sup>) from the six major rivers in the area (Pamba, Manimala, Achancoil, Meenchil, Periyar and Muvattupuzha Rivers) during the monsoon season<sup>27,28</sup> and also receives inputs

Pearson correlation			
Parameters	N <sub>2</sub> O flux Wanninkhof (1992)	N <sub>2</sub> O flux Raymond and Cole (2001)	N <sub>2</sub> O flux Wanninkhof and McGillis (1999)
Rainfall	r = 0.463, $\rho = 0.023$	Not significant (N.S.)	r = 0.501, $\rho = 0.013$
Wind speed	r = 0.827, $\rho < 0.001$	r = 0.634, $\rho = 0.001$	r = 0.790, $\rho < 0.001$
Estuarine depth	r = 0.670, $\rho < 0.001$	r = 0.567, $\rho = 0.004$	r = 0.696, $\rho < 0.001$
Salinity	r = - 0.484, $\rho = 0.017$	N.S.	r = - 0.505, $\rho = 0.012$
DO	r = - 0.516, $\rho = 0.010$	N.S.	r = - 0.554, $\rho = 0.005$
AOU	r = 0.528, $\rho = 0.009$	N.S.	r = 0.570, $\rho = 0.004$
TC (water)	r = 0.467, $\rho = 0.022$	N.S.	r = 0.494, $\rho = 0.014$
TIC (water)	r = 0.481, $\rho = 0.017$	N.S.	r = 0.504, $\rho = 0.012$
TN (water)	r = 0.664, $\rho < 0.001$	r = 0.573, $\rho = 0.003$	r = 0.690, $\rho < 0.001$
DN (water)	r = 0.701, $\rho < 0.001$	r = 0.611, $\rho = 0.002$	r = 0.726, $\rho < 0.001$
NH <sub>4</sub> (water)	N.S.	N.S.	r = 0.434, $\rho = 0.034$
NO <sub>3</sub> (water)	r = 0.617, $\rho = 0.001$	r = 0.523, $\rho = 0.009$	r = 0.638, $\rho = 0.001$
DIN (water)	r = 0.612, $\rho = 0.001$	r = 0.496, $\rho = 0.014$	r = 0.640, $\rho = 0.001$
PN (water)	r = 0.482, $\rho = 0.017$	r = 0.400, $\rho = 0.053$	r = 0.505, $\rho = 0.012$
DON (water)	r = 0.700, $\rho < 0.001$	r = 0.614, $\rho = 0.001$	r = 0.725, $\rho < 0.001$
Dissolved N <sub>2</sub> O	r = 0.654, $\rho < 0.001$	r = 0.813, $\rho < 0.001$	r = 0.590, $\rho = 0.002$
N <sub>2</sub> O saturation	r = 0.654, $\rho = 0.001$	r = 0.813, $\rho < 0.001$	r = 0.590, $\rho = 0.003$

**Table 2.** Relationship of N<sub>2</sub>O flux calculated using different models to other environmental parameters observed in the Mangalavanam Coastal Wetland, India during the study.

of approximately 260 m<sup>3</sup> of domestic and 104 × 10<sup>3</sup> m<sup>3</sup> of industrial waste discharges daily, most of which are unprocessed<sup>29,30</sup>. The CES (and subsequently the MCW) receives high inputs of N from the surrounding agricultural areas which are flushed into receiving waters (both from surface runoff and groundwater inputs). There were significant relationships between rainfall distribution pattern and NH<sub>4</sub> (r = 0.415,  $\rho = 0.044$ ), NO<sub>2</sub> (r = 0.489,  $\rho = 0.015$ ), NO<sub>3</sub> (r = 0.755,  $\rho = 0.000$ ) concentrations and N<sub>2</sub>O flux calculated using Wanninkhof<sup>15</sup> (Table 2). Similar observations of increased N loads and associated N<sub>2</sub>O fluxes due to rainfall have been reported in the eutrophic Taihu Lake in China<sup>31</sup>. The high resident time of the water column in the study lead to greater accumulation of N in the water column and longer processing times of N before being exported which likely influence N<sub>2</sub>O production and flux rates in the study area.

High N and organic carbon concentrations have been shown to accelerate the nitrification–denitrification processes<sup>31–33</sup> and lead to higher N<sub>2</sub>O production although C and N concentrations did not show a clear relationship to dissolved N<sub>2</sub>O concentration in the MCW. Non-significant relationships between dissolved N<sub>2</sub>O concentration and DIN have been observed in other recent studies<sup>34–36</sup>. However, during this study significant relationships were observed between TC, TIC, TN, DN, DIN, NO<sub>3</sub>, NH<sub>4</sub>, DON, PN and N<sub>2</sub>O flux calculated using Wanninkhof<sup>15</sup> (Table 2). This indicates a consistent relationship existed between N, C inputs and N<sub>2</sub>O outputs. Significant relationships between DIN inputs and N<sub>2</sub>O fluxes have also been shown in the nearby CES in India<sup>19</sup>, rivers<sup>37</sup> and estuaries globally<sup>38</sup>. Positive relationships were also observed between N<sub>2</sub>O and NH<sub>4</sub> and NO<sub>3</sub> + NO<sub>2</sub> during the summer dry season, while during winter, N<sub>2</sub>O saturation was strongly correlated to NO<sub>3</sub> + NO<sub>2</sub> but not with NH<sub>4</sub><sup>11</sup>.

The significant positive correlation between NO<sub>3</sub> and NH<sub>4</sub> concentrations to N<sub>2</sub>O flux calculated using Wanninkhof<sup>15</sup> and strong negative correlation between DO and NH<sub>4</sub> (r = - 0.558,  $\rho = 0.005$ ), NO<sub>2</sub> (r = - 0.586,  $\rho = 0.003$ ) and NO<sub>3</sub> (r = - 0.788,  $\rho < 0.001$ ) suggest high N<sub>2</sub>O flux rates produced through nitrification. However, lower DO during the monsoon months along with higher availability of NO<sub>3</sub> in the presence of high organic carbon loading likely promotes denitrification increasing N<sub>2</sub>O production and its fluxes. Several studies suggest that estuaries receiving higher N inputs generally show oxygen depletion, which in turn triggers denitrification<sup>34,39,40</sup>. Increasing anthropogenic nitrogen inputs to the mangrove sediments along with periodic tidal flooding can generate anoxic conditions in the sediment; thereby further enhancing denitrification<sup>41</sup>. This process along with nitrification could significantly contribute to nutrient turnover and N<sub>2</sub>O production in mangroves. However, the magnitude at which a wetland can act as source of N<sub>2</sub>O cannot be explained solely based on N loads as the magnitude of N<sub>2</sub>O flux depends on both denitrification–nitrification rates (how efficiently N is cycled) and N<sub>2</sub>O reduction rates (how efficiently N<sub>2</sub>O is reduced to N<sub>2</sub>)<sup>31</sup>.

The highest dissolved N<sub>2</sub>O concentrations and saturations were observed during the pre-monsoon season when temperatures were highest, while the N<sub>2</sub>O flux rates were highest during monsoon season. However, there was no significant relationship between water column and sediment temperatures and N<sub>2</sub>O concentrations, saturations and flux rates. Recent studies suggest that higher temperatures during summer seasons (pre-monsoon) can enhance microbial activity favouring N<sub>2</sub>O production<sup>9</sup>, while the reduced freshwater discharge during summers can increase the resident time of the water column, leading to greater accumulation of N<sub>2</sub>O in water and reducing the N<sub>2</sub>O loss to the atmosphere due to the decrease in gas transfer velocity<sup>42</sup>.

The shallow depth profile of the MCW likely promoted easier diffusion of oxygen molecules into the water column and to the sediments, favouring nitrification. This can drive higher dissolved N<sub>2</sub>O concentrations and

its saturation during the pre-monsoon than the monsoon and post-monsoon seasons. A recent report suggests that the shallow bathymetry of the CES favoured easier exchange of  $N_2O$  that was produced in the estuarine sediment and water column to the atmosphere<sup>49</sup>. A positive correlation between water column depth and  $N_2O$  flux was observed using all models (Table 2). The deepest water column depth was mainly observed during monsoon season when the C and N loads were highest; there was low DO saturation and wind speeds were highest. However the mean water column depth during the monsoon season remained shallow (less than 0.5 m) even though it had the highest range in depths (0.3–0.5 m). Combined with the higher wind speeds during the monsoon season, this resulted in higher  $N_2O$  fluxes rates. The significant negative correlation between salinity and  $N_2O$  flux calculated using Wanninkhof<sup>15</sup> was likely driven by either nutrient rich seawater returned from the CES or the reduced solubility of gases in saline conditions.

During the study, DON was the major constituent of the N and signified that the N enrichment in the study area was mainly through organic matter inputs or oceanic inputs where DON is the most prevalent form of N. As the major source of organic carbon in the study area was likely from mangrove litter which is generally nitrogen deficient<sup>43,44</sup>, the positive correlation of TC to DON in the water column ( $r = 0.870$ ,  $p < 0.001$ ) suggests that the study area receives significant amount of organic inputs from allochthonous sources, particularly with high N concentrations. The significant positive correlation between TC and TIC in the water column and  $N_2O$  flux indicates that the  $N_2O$  production and higher fluxes occurs in N rich environments with regard to C availability. However, the study failed to explain the relationship of TOC to  $N_2O$  production and fluxes. A recent study in the tropical estuaries of north-western Borneo<sup>45</sup> also failed to explain the significant correlation between DOC and  $N_2O$  concentrations. Although temperature and pH are important factors affecting  $N_2O$  production, no clear relationship was found between these variables and dissolved  $N_2O$  concentrations and fluxes. Several studies also suggest that the influence of water temperature on the denitrification rate may vary between regions and seasons<sup>31,46,47</sup>.

As the MCW is a fragmented mangrove, its atmospheric contribution of  $N_2O$  calculated using Wanninkhof<sup>15</sup> is quite small (ranging from  $1.1 \pm 0.2 \times 10^6 \mu\text{mol day}^{-1}$  during post-monsoon season to  $2.4 \pm 1.2 \times 10^6 \mu\text{mol day}^{-1}$  during monsoon season) and on its own may not be significant. However considering the numerous smaller mangrove stands that exist all over the tropics, fragmented mangroves may represent a significant source of  $N_2O$  to the atmosphere. For example, the Ernakulam district in the state Kerala alone has about 933 minor mangrove stands, covering a total area of 206 hectares. This suggests that fragmented/minor mangrove stands may have an as yet unquantified but significant influence on atmospheric  $N_2O$  budgets and atmospheric warming into the future.

## Conclusion

The net  $N_2O$  flux from MCW suggest that it is a source of atmospheric  $N_2O$ , however due to its small area of coverage its contribution to atmospheric  $N_2O$  is minor. The high precipitation rates in the study, through terrestrial runoff and river water discharge and high N inputs, influenced  $N_2O$  flux rates particularly during monsoon season. The study suggests that when taken as whole, fragmented/minor mangroves which are abundant in tropical regions, need to be critically assessed and protected from further anthropogenic loading. Further studies in a range of different geologic and hydrologic conditions will help to include this potentially significant ecosystem type in global  $N_2O$  budgets. The study highlights that  $N_2O$  flux rates were dependant on the availability of DIN as well as salinity, DO, estuarine depth, rainfall, wind speed and availability of carbon.

## Materials and methods

Field work was carried out over a period of 12 months from June 2014 to May 2015 with observations made during the morning hours on a monthly basis. Rainfall data was obtained from the Indian Meteorological Department. The depth of the wetland was measured by lowering a graduated weighted rope until it touched the top of the sediments. Transparency was measured using a 20 cm diameter Secchi disc<sup>48</sup>. Triplicates of nutrient samples were collected from surface waters at each site. Temperature, salinity and pH were measured using an Eutech water quality analyser (CyberScan Series SCD 650). Water samples for DO were taken in 60 ml glass bottles fixed with 0.5 ml each of Winkler reagents and titrated against sodium thiosulphate using visual endpoint detection<sup>49</sup>. Apparent oxygen utilisation (AOU) was calculated as outlined by Garcia and Gordon<sup>50</sup>, using the measured DO concentration. Dissolved inorganic nitrogen (DIN, which includes  $NH_4$ ,  $NO_2$ , and  $NO_3$ ) were analysed spectrophotometrically following standard procedures<sup>51</sup>.

Water samples for total organic carbon (TOC) and total inorganic carbon (TIC), total nitrogen (TN), dissolved nitrogen (DN) and dissolved  $N_2O$  were collected in 120 ml glass bottles. The samples were fixed using saturated mercuric chloride (0.6 ml/120 ml) to arrest microbial activity<sup>52</sup>. An aliquot of each sample was filtered through a 25 mm GF/F filter and the filtrate was collected for the measurement of DN, while the remainder of the sample was analysed for TOC, TIC and TN by wet combustion method using a TOC elemental analyser (Multi N/C 2100 S Analytik jena). Particulate nitrogen (PN) and dissolved organic nitrogen (DON) concentrations in the water column were calculated by subtracting DN from TN and DIN from DN, respectively.

Sediment samples were obtained using a van-Veen grab sampler (area 0.04 m<sup>2</sup>) with a glass corer (3 cm diameter) inserted into each grab sample. As the surface sediment contained mangrove litter, samples were collected at a depth of 2 cm from the surface of the sediment and sieved (usually < 2 mm), dried at 60 °C for 24–72 h and ground to a fine powder. An aliquot of the dried sediment sample was acidified using 1 M hydrochloric acid to remove the inorganic carbon present in the sample<sup>53</sup>. The acidified samples were then washed with distilled water, dried and ground to powder. The samples were then analysed for TOC using dry combustion method (TOC elemental analyser Multi N/C 2100 S, Analytik jena). The other part of the sample that was not treated with acid was used to measure TN in the sediment using Pyro-cube IRMS.

Dissolved  $N_2O$  was determined by the multiple phase equilibration technique<sup>54</sup>.



The  $N_2O$  water to air exchange fluxes ( $f$ ) were computed using:

$$f = k\alpha(C_w - C_a), \quad (1)$$

where  $k$  is the gas transfer coefficient of  $N_2O$ <sup>23,55</sup>,  $\alpha$  is the solubility coefficient of  $N_2O$  calculated using temperature and salinity<sup>56</sup>,  $C_w$  is the water column  $N_2O$  partial pressure and  $C_a$  is the local measured atmospheric value for  $N_2O$  (323 ppb as recently reported)<sup>57</sup>. To provide a comparison of different  $k$  values, the wind parameterization  $k$  models of Wanninkhof<sup>15</sup>, Wanninkhof and McGillis<sup>16</sup> and Raymond and Cole<sup>17</sup> were calculated. Wind speed data (10 m height) were obtained from ERA interim, European Centre for Medium Range Weather Forecast (ECMWF) with a data resolution of ~ 80 km from the study site.

SPSS v16 (Statistical Programme for Social Sciences v16) was used for Pearson's correlation analyses and the two-way analysis of variance (ANOVA) and Origin Pro 8.5 used to plot the graphs.

## Data availability

Most of the data generated during the current study is graphically represented in the manuscript. The datasets generated during and/or analysed during the current study are also available from the corresponding author on reasonable request.

Received: 28 May 2020; Accepted: 15 February 2021

Published online: 25 March 2021

## References

- Kroeze, C., Dumont, E. & Seitzinger, S. P. New estimates of global emissions of  $N_2O$  from rivers and estuaries. *Environ. Sci.* **2**(2–3), 159–165. <https://doi.org/10.1080/15693430500384671> (2005).
- Ciais, P. *et al.* Carbon and other biogeochemical cycles. In *Climate Change 2013: The Physical Science Basis. Contribution of Working Group I to the Fifth Assessment Report of the Intergovernmental Panel on Climate Change* 465–570 (Cambridge University Press, 2014).
- Forster, P. *et al.* Changes in atmospheric constituents and in radiative forcing. Chapter 2. In *Climate Change 2007. The Physical Science Basis* (2007).
- Butterbach-Bahl, K., Baggs, E. M., Dannenmann, M., Kiese, R. & Zechmeister-Boltenstern, S. Nitrous oxide emissions from soils: How well do we understand the processes and their controls?. *Philos. Trans. R. Soc. B.* <https://doi.org/10.1098/rstb.2013.0122> (2013).
- Reis, C. R. G., Nardoto, G. B. & Oliveira, R. S. Global overview on nitrogen dynamics in mangroves and consequences of increasing nitrogen availability for these systems. *Plant Soil.* **410**(1–2), 1–19. <https://doi.org/10.1007/s11104-016-3123-7#citeas> (2017).
- Rao, K., Priya, N. & Ramanathan, A. L. Impacts of anthropogenic perturbations on reactive nitrogen dynamics in mangrove ecosystem: Climate change perspective. *J. Clim. Change* **5**(2), 9–21 (2019).
- Centre for Coastal Zone Management and Coastal Shelter Belt, Ministry of Environment, Forests and Climate change, Govt. of India <http://iomenvis.nic.in/index2.aspx?slid=758&sublinkid=119&langid=1&mid=1> (2017).
- FSI. India State of Forest Report. 2019. Forest Survey of India, Ministry of Environment and Forests, Dehradun (2019).
- Borges, A. V. *et al.* Effects of agricultural land use on fluvial carbon dioxide, methane and nitrous oxide concentrations in a large European river, the Meuse (Belgium). *Sci. Total Environ.* **610**, 342–355. <https://doi.org/10.1016/j.scitotenv.2017.08.047> (2018).
- Lin, H. *et al.* Spatiotemporal variability of nitrous oxide in a large eutrophic estuarine system: The Pearl River Estuary, China. *Mar. Chem.* **182**, 14–24. <https://doi.org/10.1016/j.marchem.2016.03.005> (2016).
- Reading, M. J. *et al.* Land use drives nitrous oxide dynamics in estuaries on regional and global scales. *Limnol.* **65**(8), 1903–1920. <https://doi.org/10.1002/lno.11426> (2020).
- Chauhan, R., Ramanathan, A. L. & Adhya, T. K. Assessment of methane and nitrous oxide flux from mangrove along Eastern coast of India. *Geofluids* **8**, 321332. <https://doi.org/10.1111/j.1468-8123.2008.00227.x> (2008).
- Kriethika, K., Purvaja, R. & Ramesh, R. Fluxes of methane and nitrous oxide from an Indian mangrove. *Curr. Sci.* **94**, 218224, <https://www.jstor.org/stable/24101861> (2008).
- Fernandes, S. O., LokaBharathi, P. A., Bonin, P. C. & Michotey, V. D. Denitrification: An important pathway for nitrous oxide production in tropical mangrove sediments (Goa, India). *J. Environ. Qual.* **39**, 1507–1516. <https://doi.org/10.2134/jeq2009.0477> (2010).
- Wanninkhof, R. Relationship between wind speed and gas exchange over the ocean. *J. Geophys. Res.* **97**, 7373–7382. <https://doi.org/10.4319/lom.2014.12.351> (1992).
- Wanninkhof, R. & McGillis, W. M. A cubic relationship between gas transfer and wind speed. *Geophys. Res. Lett.* **26**, 1889–1893. <https://doi.org/10.1029/1999GL900363> (1999).
- Raymond, P. A. & Cole, J. J. Gas exchange in rivers and estuaries: Choosing a gas transfer velocity. *Estuaries* **24**, 312–317. <https://doi.org/10.2307/1352954> (2001).
- Hershey, R. N., Nandan, S. B. & Vasu, N. K. Trophic status and nutrient regime of Cochin estuarine system, India. *Indian J. Mar. Sci.* **49**(08), 2582–6727 <http://nopr.niscair.res.in/handle/123456789/55309> (2020).
- Hershey, R. N. *et al.* Nitrous oxide flux from a Tropical estuarine system (Cochin estuary, India). *Reg. Stud. Mar. Sci.* **30**, 100725. <https://doi.org/10.1016/j.rsma.2019.100725> (2019).
- Maher, D. T., Sippo, J. Z., Tait, D. R., Holloway, C. & Santos, I. R. Pristine mangrove creek waters are a sink of nitrous oxide. *Sci. Rep.* **6**, 25701. <https://doi.org/10.1038/srep25701> (2016).
- Tait, D. R. *et al.* Greenhouse gas dynamics in a salt-wedge estuary revealed by high resolution cavity ring-down spectroscopy observations. *Environ. Sci. Technol.* **51**(23), 13771–13778. <https://doi.org/10.1021/acs.est.7b04627> (2017).
- Wells, N. S. *et al.* Estuaries as sources and sinks of  $N_2O$  across a land use gradient in subtropical Australia. *Glob. Biogeochem. Cycles.* **32**, 877–894. <https://doi.org/10.1029/2017GB005826> (2018).
- Upstill-Goddard, R. C. Air–sea gas exchange in the coastal zone. *Estuar Coast Shelf Sci.* **70**, 388–404. <https://doi.org/10.1016/j.ecss.2006.05.043> (2006).
- Zappa, C. J., Raymond, P. A., Terray, E. A. & McGillis, W. R. Variation in surface turbulence and gas transfer velocity over a tidal cycle in a macro-tidal estuary. *Estuaries* **26**, 1401–1415. <https://doi.org/10.1007/BF02803649#citeas> (2003).
- Borges, A. V. *et al.* Gas transfer velocities of  $CO_2$  in three European estuaries (Randers Fjord, Scheldt, and Thames). *Limnol. Oceanogr.* **49**, 1630–1641. <https://doi.org/10.4319/lo.2004.49.5.1630> (2004).
- Munoz-Hincapie, M., Morell, J. M. & Corredor, J. E. Increase of nitrous oxide flux to the atmosphere upon nitrogen addition to red mangroves sediments. *Mar. Pollut. Bull.* **44**, 992–996. [https://doi.org/10.1016/S0025-326X\(02\)00132-7](https://doi.org/10.1016/S0025-326X(02)00132-7) (2002).

27. Srinivas, K., Revichandran, P., Maheswaran, P. A., Mohammed Ashraf, T. T. & Nuncio, M. Propagation of tides in the Cochin estuarine system, southwest coast of India. *Indian J. Geomar. Sci.* **32**(1), 14–24 (2003).
28. Srinivas, K., Revichandran, C. & Dinesh Kumar, P. K. Statistical forecasting of met-ocean parameters in the Cochin estuarine system, southwest coast of India. *Indian J. Geomar. Sci.* **32**(4), 285–293 (2003).
29. Balachandran, K. K., Joseph, T., Nair, K. K. C., Nair, M. & Joseph, P. S. The complex estuarine formation of six rivers (Cochin backwaters system on westcoast of India)—Sources and distribution of trace metals and nutrients. In: APN/SASCOM/LOICZ Regional Workshop on Assessment of Material Fluxes To the Coastal Zone in South Asia and their Impacts. Sri Lanka National Committee of IGBP, Colombo, Sri Lanka, 359, <http://drs.nio.org/drs/handle/2264/1340> (2002).
30. Martin, G. D. *et al.* Freshwater influence on nutrient stoichiometry in a tropical estuary, southwest coast of India. *Appl. Ecol. Environ. Res.* **6**, 57–64 (2008).
31. Liu, D. *et al.* N<sub>2</sub>O fluxes and rates of nitrification and denitrification at the sediment-water interface in Taihu Lake, China. *Water* **10**, 911. <https://doi.org/10.3390/w10070911> (2018).
32. Luijn, F. V., Boers, P. C. M. & Lijklema, L. Comparison of denitrification rates in lake sediments obtained by the N<sub>2</sub> flux method, the 15N isotope pairing technique and the mass balance approach. *Water Res.* **30**, 893–900. [https://doi.org/10.1016/0043-1354\(95\)00250-2](https://doi.org/10.1016/0043-1354(95)00250-2) (1996).
33. Pfenning, K. S. & McMahon, P. B. Effect of nitrate, organic carbon, and temperature on potential denitrification rates in nitrate-rich riverbed sediments. *J. Hydrol.* **187**, 283–295. [https://doi.org/10.1016/S0022-1694\(96\)03052-1](https://doi.org/10.1016/S0022-1694(96)03052-1) (1997).
34. Borges, A. V. *et al.* Globally significant greenhouse-gas emissions from African inland waters. *Nat. Geosci.* **8**(8), 637–642. <https://doi.org/10.1038/ngeo2486> (2015).
35. Marzadri, A., Dee, M. M., Tonina, D., Bellin, A. & Tank, J. L. Role of surface and subsurface processes in scaling N<sub>2</sub>O emissions along riverine networks. *Proc. Natl. Acad. Sci. U. S. A.* **114**(17), 4330–4335. <https://doi.org/10.1073/pnas.1617454114> (2017).
36. Soued, C., del Giorgio, P. A. & Maranger, R. Nitrous oxide sinks and emissions in boreal aquatic networks in Quebec. *Nat. Geosci.* **9**(2), 116–120. <https://www.x-mol.com/paperRedirect/68353> (2016).
37. Hu, M. P., Chen, D. J. & Dahlgren, R. A. Modeling nitrous oxide emission from rivers: A global assessment. *Glob. Change Biol.* **22**(11), 3566–3582. <https://doi.org/10.1111/gcb.13351> (2016).
38. Murray, R., Erler, D. V., Rosentreter, J., Wells, N. S. & Eyre, B. D. Seasonal and spatial controls on N<sub>2</sub>O concentrations and emissions in low-nitrogen estuaries: Evidence from three tropical systems. *Mar. Chem.* <https://doi.org/10.1016/j.marchem.2020.103779> (2020).
39. Ji, Q. X., Babbitt, A. R., Peng, X. F., Bowen, J. L. & Ward, B. B. Nitrogen substrate dependent nitrous oxide cycling in salt marsh sediments. *J. Mar. Res.* **73**(3–4), 71–92. <https://doi.org/10.1016/j.marchem.2020.103779> (2015).
40. Punshon, S. & Moore, R. M. Nitrous oxide production and consumption in a eutrophic coastal embayment. *Mar. Chem.* **91**(1–4), 37–51. <https://doi.org/10.1016/j.marchem.2004.04.003> (2004).
41. Corredor, J. E., Morell, J. M. & Bauza, J. Atmospheric nitrous oxide fluxes from mangrove sediments. *Mar. Pollut. Bull.* **38**, 473–478. [https://doi.org/10.1016/S0025-326X\(98\)00172-6](https://doi.org/10.1016/S0025-326X(98)00172-6) (1999).
42. Raymond, P. A. *et al.* Scaling the gas transfer velocity and hydraulic geometry in streams and small rivers. *Limnol. Oceanogr. Fluids Environ.* **2**, 41–53. <https://doi.org/10.1215/21573689-1597669> (2012).
43. Alongi, D. M. Impact of global change on nutrient dynamics in mangrove forests. *Forests.* **9**(10), 596. <https://doi.org/10.3390/f9100596> (2018).
44. Reef, R., Feller, I. C. & Lovelock, C. E. Nutrition of mangroves. *Tree Physiol.* **30**, 1148–1160. <https://doi.org/10.1093/treephys/tpq048> (2010).
45. Muller, D. *et al.* Nitrous oxide and methane in two tropical estuaries in a peat-dominated region of northwestern Borneo. *Biogeosciences* **13**(8), 2415–2428. <https://doi.org/10.5194/bg-13-2415-2016> (2016).
46. Hasegawa, T. & Okino, T. Seasonal variation of denitrification rate in Lake Suwa sediment. *Limnology* **5**(1), 33–39. <https://doi.org/10.1007/PL00021725/citeas> (2004).
47. Myrstener, M., Jonsson, A. & Bergström, A. K. The effects of temperature and resource availability on denitrification and relative N<sub>2</sub>O production in boreal lake sediments. *J. Environ. Sci. (China)*.
48. Strickland, J. D. H. & Parsons, T. R. *A Practical Handbook of Seawater Analysis*. 2nd edn. 310 (Fisheries Research Board of Canada, 1972).
49. Grasshoff, K., Ehrhardt, M. & Kremling, K. *Methods of seawater analysis*. 2nd edn. 419 (Verlag Chemie, 1983).
50. Garcia, H. & Gordon, L. Oxygen solubility in seawater: Better fitting equations. *Limnol. Oceanogr.* **37**, 1307–1312. <https://doi.org/10.4319/lo.1992.37.6.1307> (1992).
51. Grasshoff, K., Ehrhardt, M. & Kremling, K. *Methods of Seawater Analysis* 3rd edn. (VCH, 1999).
52. David, A. R. Analysis of Total organic carbon. UMass Environmental Engineering Program (2012).
53. Polunin, N. V. *et al.* Feeding relationships in Mediterranean bathyal assemblages elucidated by stable nitrogen and carbon isotope data. *Mar. Ecol. Prog. Ser.* **220**, 13–23. <https://doi.org/10.3354/meps220013> (2001).
54. McAuliffe, C. GC determination of solutes by multiple phase equilibrations. *Chem. Tech.* **1**, 46–50 (1971).
55. Liss, P. S. & Merlivat, L. Air-sea exchange rates: Introduction and synthesis, in the role of air-sea exchange in geochemical cycling. In (ed. Buat-Menard, P.) 113–127 (D Reidel, 1986) [https://doi.org/10.1007/978-94-009-4738-2\\_5](https://doi.org/10.1007/978-94-009-4738-2_5).
56. Weiss, R. F. & Price, B. A. Nitrous oxide solubility in water and seawater. *Mar. Chem.* **8**, 347–359. [https://doi.org/10.1016/0304-4203\(80\)90024-9](https://doi.org/10.1016/0304-4203(80)90024-9) (1980).
57. Rao, G. D., Rao, V. D. & Sarma, V. V. S. S. Distribution and air–sea exchange of Nitrous oxide in the Coastal Bay of Bengal during peak discharge period(southwest monsoon). *Mar. Chem.* **155**, 1–9. <https://doi.org/10.1016/j.marchem.2013.04.014> (2013).

## Acknowledgements

We would like to thank Department of Environment and Climate Change, Govt. of Kerala and University Grant Commission for financial support, Department of Marine Biology, Microbiology and Biochemistry, Cochin University of Science and Technology, Kerala for the facility and support. We are also grateful to Mr. Aravind E.H., and Dr. Preethy C.M., Department of Marine Biology, Microbiology and Biochemistry, Cochin University of Science and Technology, Kerala and Dr. Ruchith R.D., Scientist- B, NIO (Goa) for their valuable support.

## Author contributions

Study design: S.B.N. and R.H.N. Field work and sample analysis: R.H.N. and N.V.K. Data analysis: R.H.N. and D.R.T. Manuscript preparation: R.H.N. Reviewers: D.R.T., S.B.N., R.H.N.

## Competing interests

The authors declare no competing interests.

### Additional information

**Correspondence** and requests for materials should be addressed to S.B.N.

**Reprints and permissions information** is available at [www.nature.com/reprints](http://www.nature.com/reprints).

**Publisher's note** Springer Nature remains neutral with regard to jurisdictional claims in published maps and institutional affiliations.



**Open Access** This article is licensed under a Creative Commons Attribution 4.0 International License, which permits use, sharing, adaptation, distribution and reproduction in any medium or format, as long as you give appropriate credit to the original author(s) and the source, provide a link to the Creative Commons licence, and indicate if changes were made. The images or other third party material in this article are included in the article's Creative Commons licence, unless indicated otherwise in a credit line to the material. If material is not included in the article's Creative Commons licence and your intended use is not permitted by statutory regulation or exceeds the permitted use, you will need to obtain permission directly from the copyright holder. To view a copy of this licence, visit <http://creativecommons.org/licenses/by/4.0/>.

© The Author(s) 2021